Density Coordinate Mixed Layer Models

WILLIAM K. DEWAR

Department of Oceanography and School of Computational Science and Information Technology, The Florida State University, Tallahassee, Florida

(Manuscript received 14 July 1999, in final form 3 April 2000)

ABSTRACT

The development of mixed layer models in so-called density coordinates is discussed. Density coordinates, or isopycnal coordinates as they are sometimes called, are becoming increasingly popular for use in ocean models due to their highly desirable adiabatic properties. In contrast, almost all existing mixed layer models assume a continuous density variable and are therefore somewhat inconsistent with the density coordinate philosophy. Many existing isopycnal models attempt to join standard surface mixed layer models to density coordinate interior models, and it is known that problems can arise in the physical behavior of the resulting system. The problem of mixed layer model development is approached here by adopting a density coordinate framework at the outset, thereby generating a surface layer model whose construction is entirely consistent with that of existing interior density coordinate models. Examples of quantitative and qualitative behavior are presented and argued to be encouraging.

1. Introduction

The last decade has seen an enormous increase in the number, type, and use of ocean models. Several choices are implicit in the construction of any one model, including the coordinates in which the model is cast. Among the coordinate options are traditional ''*z* coordinates (or geopotential coordinates),'' sigma (bottom following) coordinates, and density, or ''isopycnal,'' coordinates. The latter is an example of a quasi-Lagrangian coordinate model where the vertical coordinate is not fixed in space: isopycnal models use isopycnal surfaces for their vertical coordinate. Recently interest has grown in the use of isopycnal models for global simulation, but to do so requires interfacing the isopycnal interior to the surface mixed layer. Traditional mixed layer models are based on a continuous surface density variable and thus are fundamentally inconsistent with isopycnal models. The objective of this paper is to explore the development of a mixed layer model composed in isopycnal coordinates, for the reason that such a model would not suffer from this inconsistency.

Background

The inclusion of stratification in ocean models by stacking layers of differing density has a long history. Phillips (1951) proposed what is perhaps the first such model, and since then, the use of layered models in geophysical fluid dynamics has become routine. The success of such models in process studies can be at least partly ascribed to the fact that many interesting ocean phenomena are essentially adiabatic.

Ocean simulation, in contrast, requires the accurate modeling of thermodynamics. If one adopts potential density as a vertical coordinate, as isopycnal models do, then the vertical coordinate is cast as a function of the two quantities potential temperature, θ, and salinity, S. Both of these are conservative quantites and in the absence of mixing, fluid parcels are required by construction to move on isopycnal surfaces. Recent direct measurements of diapycnal flux made during the North Atlantic Tracer Release Experiment (NATRE; Ledwell et al. 1993) combined with other dissipation-based estimates of diapycnal diffusivity argue that the ocean interior mixes less than previously thought. Aside from subtleties involving the full nonlinear equation of state, isopycnal models capture this adiabatic nature very effectively and have therefore gained in popularity as a tool for ocean simulation.

The value of this adiabatic nature should not be underestimated. Indeed, the problems inherent in mixing representations in classical geopotential coordinate based models have been known for some time (Veronis 1975). Some recent advances in the parameterization of tracer transport (Gent and McWilliams 1990; Griffies et al. 1998) have solved the problem of subgrid-scale diapycnal transport error in geopotential coordinate mod-

Corresponding author address: Prof. William K. Dewar, Department of Oceanography, The Florida State University, Tallahassee, FL 32306-4320.
E-mail: dewar@ocean.fsu.edu

els, but Griffies et al. (2000) have recently shown that errors in advection schemes can generate spurious diapycnal diffusion.

The related difficulties encountered with isopycnal models lie in the opposite extreme; it is the inclusion of diabatic processes that is problematic. Yet, ocean simulation requires models that can accommodate an enormous range of diabatic conditions. The ocean interior, while largely conservative of heat and salt, stands in contrast to the surface layers where essential exchanges of mass and heat take place. Classical mixed layer models predict mixed layer potential temperature and salinity as functions of buoyancy inputs. The mixed layer density diagnosed from the θ and S need not occur on any preselected subset of densities, so at some level, such mixed layer surface models are inconsistent with isopycnal models of the subsurface. On the other hand, there is a considerable literature on this type of mixed layer modeling (e.g., Kraus and Turner 1967; Niiler and Kraus 1977; Price et al. 1986; Gaspar 1988; Large et al. 1994), and the predictive skill of such models is now quite advanced.

One possible solution to the problem of ocean model construction, given these widely varying mixing requirements, is to produce a hybrid model, in which the model type is fitted to given ocean regimes. For example, one might employ isopycnal coordinates for the ocean interior and a gridpoint model in the mixed layer. The transition between the two could be mediated by a stack of hybrid coordinates that smoothly change from one to the other in the near-surface zone. Sigma bottom-following coordinates might compose the deepest reaches of the model. Indeed, such a philosophy has underpinned some recent model development [e.g., the National Aeronautics and Space Administration (NASA) Poseidon Ocean Model; see Schopf and Loughe (1995) and Murtugudde et al. (1995)]. A related approach, which has a bit more history behind it, involves patching traditional continuous density mixed layer models directly to the discretely resolved density coordinate interior. Examples are the Miami Isopycnal Coordinate Ocean Model (Bleck and Chassignet 1994), and the Oberhuber model (Oberhuber 1993).

The hybrid coordinate approach, currently in the developmental stage, may turn out to be a viable and accurate method. Relative to the latter approach, there are at present some remaining unsolved numerical and physical issues. In particular, during the detraining phase of mixed layer evolution, the mixed layer leaves behind fluid of a density generally distinct from any of the interior densities. Procedures must then be implemented to redistribute the excess buoyancy in the interior in such a way that the interior target densities can be obtained while simultaneously conserving net heat and salt. This generally involves an upgradient tracer flux (e.g., transport of buoyancy from the sub–mixed layer waters toward the more buoyant mixed layer). Such a transport is hard to justify physically and can potentially impact water mass properties.

An alternative approach to ocean model construction is to investigate whether any one single coordinate choice can be optimized to operate under the broad range of oceanic conditions. This is the principle motivation for the present work where we examine mixed layer models and their expression in density coordinates. This is an approach that has little to no literature behind it, but in principle, a mixed layer model designed wholly within density coordinates would avoid many of the essentially unphysical numerical difficulties mentioned above. Such a model, to be considered for use in ocean simulation, must at least be able to admit arbitrary surface fluxes of heat and freshwater as well as penetrative solar radiation and must also be able to transition smoothly to a density coordinate interior without unphysical tracer fluxes or spurious mixing. In addition, it should be perfectly conservative in heat and salt and viable in the presence of a nonlinear equation of state. Of these several requirements, we consider all but the last, which is a general concern for mixing in isopycnal models. The first several issues introduce a number of new considerations into mixed layer modeling in isopycnal coordinates and are isolated here for the sake of clarity.

Below, we outline the theoretical basis for a density coordinate mixed layer model and discuss some of the related difficulties. Accordingly, the model is founded on existing theoretical, experimental, and analytical insights into mixing in layered fluids, but we find it necessary to generalize some of the concepts to admit all possible mixed layer states. In section 3, we discuss an implementation of the theory to one-dimensional test problems and compare the model behavior to that predicted by a well-known and tested mixed layer model. The qualitative and quantitative comparisons therein argue that our procedure is not without skill. A discussion section concludes the paper and sets some problems for future consideration.

2. Model development

The inclusion of diapycnal mixing in layered models was addressed recently in Hu (1996) and McDougall and Dewar (1998, MD98 hereafter). In the latter, it was argued that a scheme based on the physical model of dual-sided entrainment possessed most all of the properties that one would like in a numerical model of mixing. These included exact conservation of heat and salt, conservation of coordinate, and the ability to accommodate a variety of boundary conditions, among others. Further, the levels of mixing were placed entirely in the hands of the modeler.

The present model will be based on the MD98 mixing model, although generalization will be necessary for the scheme to handle the decidedly more complex surface mixing regime. Our goal is to compute mixed layer

evolution in the presence of surface heat exchange, penetrative solar radiation, and either freshwater flux at the surface or virtual salt flux. For the present purposes, we will use a linear equation of state. Difficulties encountered in mixing parameterizations in layered schemes caused by equation of state nonlinearities are discussed in MD98.

We adopt the convention that layers are characterized by uniform density (equivalent to uniform potential density due to our linear equation of state) and are well mixed vertically in two tracers, taken to be potential temperature (θ) and salinity (S). The model is developed in one spatial dimension (i.e., vertical), this being the simplest system in which the essential mixed layer problems are encountered, and also the one in which traditional mixed layer model formulations have been developed. We discuss extensions to three spatial dimensions in the final section.

a. Interior mixing

The equations for tracer fields are in general

$$\frac{d}{dt}\theta = -F_z^\theta \quad \text{and} \tag{1}$$

$$\frac{d}{dt}S = -F_z^S, \tag{2}$$

where $F^{(\theta,S)}$ represent the turbulent fluxes of temperature and salt and the subscript z denotes a vertical derivative. The subscript i appended to these variables implies their evaluation within layer i. Our convention is that positive temperature fluxes denote warm temperatures rising and negative temperature fluxes warm temperatures descending. A positive salinity flux denotes the downward penetration of relatively fresh (low salinity) water and negative salinity fluxes the upward movement of freshwater. Note (1) and (2) are written in z coordinates, but will be used to constrain the behavior of the tracers in our layered format.

The continuity equation yields for a layered fluid, after some algebra,

$$\frac{d}{dt}h_i = e_{i-1}^i - e_i^{i+1}, \tag{3}$$

where e_{i-1}^i denotes the net entrainment into layer i from layer $i-1$ and h_i the thickness of layer i. The index labels attached to the layer properties and interfaces appear in Fig. 1.

Our coordinate definition adds the constraint

$$\frac{d}{dt}\rho_i = -\alpha\frac{d}{dt}\theta_i + \beta\frac{d}{dt}S_i = 0 \tag{4}$$

for all layers, while the requirement of vertically uniform profiles implies

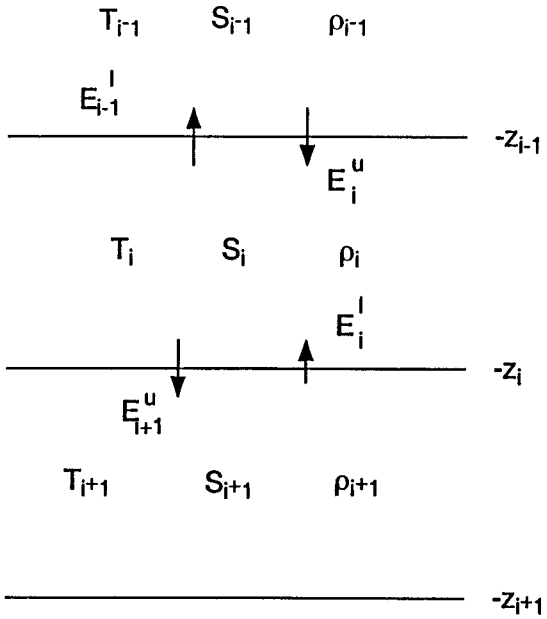

FIG. 1. Model schematic. Index i is associated with the layer properties θ, S, and h. The interfaces bounding layer i are at $z = -z_{i-1}$ above and $z = -z_i$ below. The surface occurs at $z = \eta$.

$$h_i\frac{d}{dt}\theta_i = -F_i^{\theta,u} + F_i^{\theta,l} \quad \text{and} \tag{5}$$

$$h_i\frac{d}{dt}S_i = -F_i^{S,u} + F_i^{S,l} \tag{6}$$

within layers. In the above, $F_i^{(\theta,S),u}$, $F_i^{(\theta,S),l}$ denote the [temperature, salinity] fluxes at the upper and lower interfaces of layer i, respectively.

If (1) and (2) are integrated across an interface, say z_i, the result is

$$\frac{d}{dt}z_i = -\frac{\Delta_i[F^{(\theta,S)}]}{\Delta_i[(\theta, S)]}, \tag{7}$$

where the notation $\Delta_i[X] = X_i - X_{i+1}$. Thus, the difference in tracer fluxes across an interface is related to the net entrainment across that interface through (3) and (7). This was argued in MD98 to be consistent with a dual-sided entrainment representation of mixing, where the net entrainment was equated to the difference of entrainments across the interface:

$$e_{i+1}^i = E_i^l - E_{i+1}^u. \tag{8}$$

The quantities $E_i^{(l,u)}$ represent the lower and upper entrainment rates for layer i, respectively. According to laboratory results, the one-sided entrainment rates on the right-hand side of (8) can be related to the rate at which energy is made available within the layer for mixing. If we denote the injection of energy into layer i due to mechanical stirring by u_{i*}^3, then

$$g\frac{(\rho_{i+1} - \rho_i)}{\rho_o}E_{io}^l = g_i'E_{io}^l = g_{i-1}'E_{io}^u = \kappa\frac{u_{i*}^3}{h_i}, \tag{9}$$

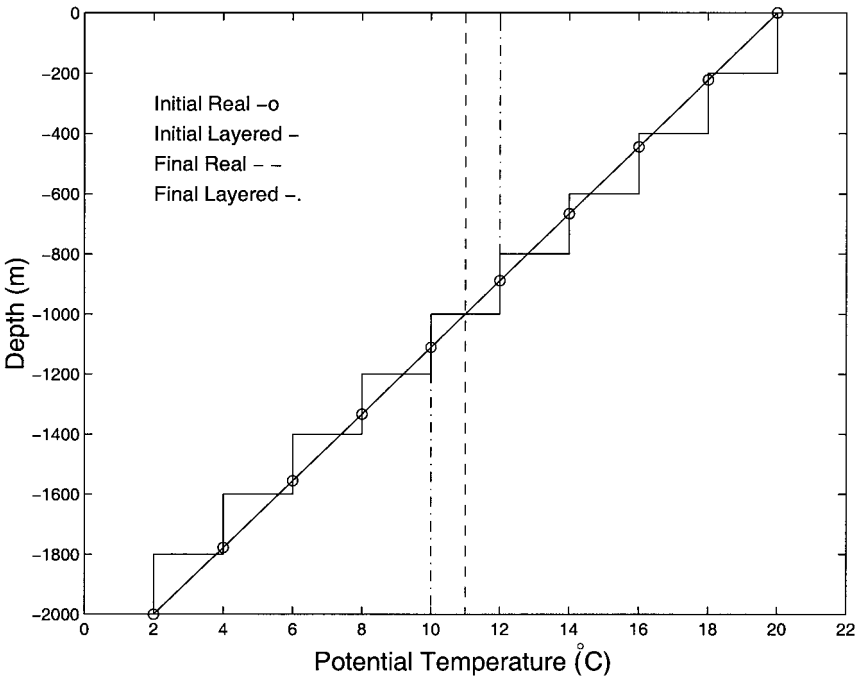

FIG. 2. An example mixing problem in layered coordinates. The fluid is considered initially as linearly stratified in potential temperature, from 20°C at the top to 2°C at 2000-m depth. The straight solid line with circles is the initial temperature profile for a real fluid and the other solid line is the same initial profile in a layered fluid. The dashed line is the real fluid end state, consisting of a well-mixed layer at 11°C. The dashed–dotted line is the final state of the layered fluid; the two layers bounding 11°C are involved. This is the analog in a layered fluid of a well-mixed layer.

where κ is a proportionality constant denoting the fraction of the provided work used to increase the layer potential energy. For layers within the fluid, the application of the above naturally met constraint (4) required by coordinate definition, as can be seen by substitution.

In the presence of a general entrainment, $E_i^{(u,l)}$, the formulas for the property fluxes become

$$F_i^{(\theta,S),u} = -E_i^u \Delta_{i-1}[(\theta, S)] \quad \text{and}$$
$$F_i^{(\theta,S),l} = -E_i^l \Delta_i[(\theta, S)], \tag{10}$$

consistent with (7). For layers neighboring boundaries, the entrainment rates had to be modified in view of the boundary conditions. Equations (9) and (10) formed the basis for the interior mixing scheme proposed by MD98 and will be used here as well to provide background mixing.

b. Mixed layer considerations

A key point in MD98 for the present work was that applying the above scheme to an initially stratified fluid, subject to insulating boundary conditions on both θ and S, generally resulted in a two-layered final state. This is illustrated in Fig. 2. The final total mass, heat, and salt in the fluid is determined by the initial mass, heat, and salt. The two final densities of the layered representation are those densities that bound the final density of the final mixed state. This totals to five constraints on six unknowns, the additional information needed to completely specify the problem comes from the time integration of the system. In any case, this thought problem demonstrates that *the analog of a well-mixed fluid in a layered system is a two-layered fluid.* The error associated with the density discretization (i.e., the difference between the layer model final densities and the true final density) decreases as the number of layers is increased, in keeping with intuition. The connection of this result to the current mixed layer model development is that we will employ the upper two layers of the model to represent the mixed layer in the system.

c. Entraining and convecting scenarios

The intuitively obvious way to introduce buoyancy fluxes into the system is through the specification of boundary conditions. In the above thought problem, the applied conditions were those of no normal flux on both boundaries. We will continue to apply no flux on the bottom for both θ and S. It is convenient to specify fluxes at the surface for θ; for S the proper boundary condition depends on whether so-called natural boundary conditions [i.e., freshwater flux; Huang (1993)] or

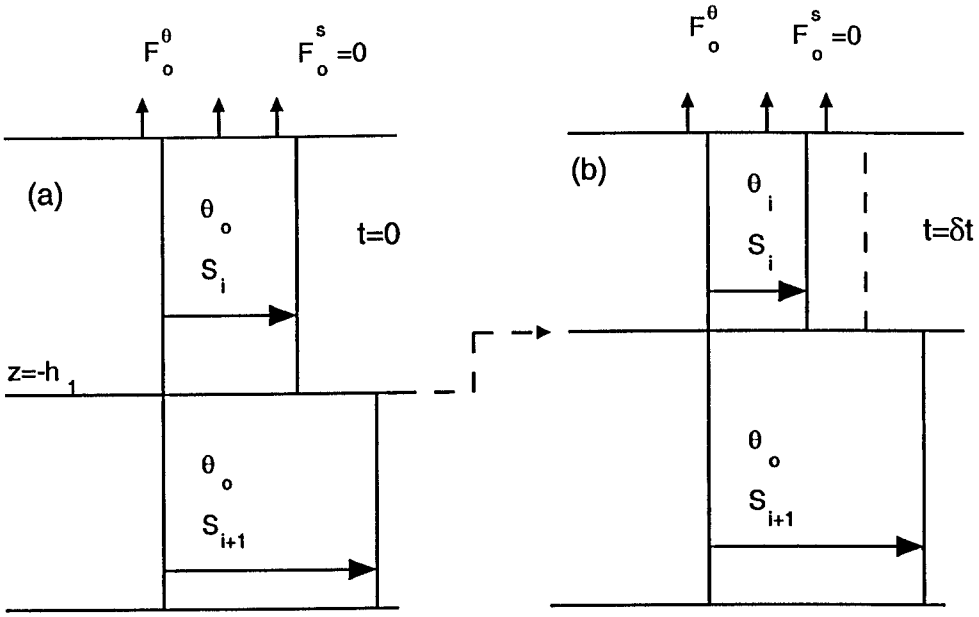

FIG. 3. Surface mixed layer schematic. (a) It is assumed the upper layer is cooled by the atmosphere under conditions of vanishing evaporation and precipitation. The two layers composing the mixed layer are assumed to be of the same temperature, and the deeper of the two of higher salinity to ensure static stability. Under these convective conditions, the normal diapycnal parameterizations predict a negative entrainment rate and, therefore, that the surface layer becomes thinner and fresher. The resultant state is depicted in (b), where the dashed line in layer i is the initial salinity.

virtual salt flux are desired. In both cases, the total surface salt flux vanishes; thus, diffusive flux must balance advective flux:

$$(e - p)S = -F^S(z = \eta), \tag{11}$$

where η is the free surface. Net moisture flux at the free surface appears in the above as $(e - p)$, representing evaporation minus precipitation. Equation (11) determines the salt flux for natural boundary conditions. To guarantee total salt conservation, the free surface must be related to $e - p$, so that the uppermost layer thickness evolves according to

$$\frac{d}{dt}h_i = -(e - p) + E_i^l - E_{i+1}^u. \tag{12}$$

Virtual salt flux boundary conditions approximate (the variable) S in (11) by a constant S_o and neglect $(e - p)$ in (12).

It has been necessary to generalize our mixing model to guarantee physically acceptable behavior in the mixed layer. The following simple example demonstrates the problems that arise if the above scheme is employed at the surface. Enforcing (4) in the presence of arbitrary surface fluxes and employing (10) leads to the formula

$$\left[\frac{\alpha F_o^\theta - \beta F_o^S}{\Delta_i[\rho]}\right] = E_i^l \tag{13}$$

for the entrainment at the surface layer base, where the surface heat and salt fluxes are denoted by F_o^θ and F_o^S, respectively. This entrainment rate guarantees conservation of the surface layer coordinate. The numerator of the left-hand side represents the buoyancy change in the layer due to the surface fluxes. For convective situations, the predicted entrainment rate is negative (i.e., the net buoyancy flux is negative and the density step is necessarily positive), and physical problems can erupt in this case.

Suppose, for example, that the surface temperature flux is positive (i.e., heat is being lost to the atmosphere), the surface salinity flux vanishes and the upper two layers have identical temperatures (see Fig. 3a). Stable stratification is assured by the $i + 1$ layer beneath the i surface layer being saltier. The parameterization as described above then predicts

$$\frac{d}{dt}h_i = E_i^l < 0,$$

$$h_i\frac{d}{dt}\theta_i = -F_o^\theta < 0, \quad \text{and}$$

$$h_i\frac{d}{dt}S_i = -E_i^l\Delta_i[S] < 0. \tag{14}$$

The latter implies the surface layer becomes fresher. The end state so described appears in Fig. 3b. Since there is no surface salinity flux, it is clear that the source of freshwater driving the surface freshening is in fact the saltier water below. This unphysical result is due to an effective ''unmixing'' driven by the negative entrain-

ment rate in (13). (On the other hand, for buoyancy injection, as would occur during summer warming conditions, the predicted entrainment rate is positive and the predicted response is acceptable.)

Since both positive and negative buoyancy fluxes into the surface are routine, a mixed layer model in density coordinates must overcome this problem if it is to be useful. The basis of our flux generalization is that the entrainment model in (10) is appropriate to stress-driven entrainment, where the entrainment of neighboring fluid into the central layer requires that buoyant resistance be overcome (i.e., the entrainment of lighter water above and/or heavier water below). In this case, energy must be supplied to the layer for entrainment to occur. For convective surface fluxes, however, this is not the case. Negatively buoyant water is produced in the surface layer, and no mechanical energy need be supplied in either the first or second layers for mixing to take place. Alternatively, one may think of the (potential) energy input into the remote surface layer as an energy source for mixing the second layer.

It is still necessary for our mixing scheme to be constrained by (1)–(3) [which jointly imply (7)]; however, these equations are consistent with a generalized tracer flux, which at the interface takes the form

$$F_i^{(\theta,S),u} = -E_i^u \Delta_{i-1}(\theta, S) + \hat{F}_{i-1}^{(\theta,S)} \quad \text{and}$$
$$F_i^{(\theta,S),l} = -E_i^l \Delta_i(\theta, S) + \hat{F}_i^{(\theta,S)}. \tag{15}$$

The above consists of an entrainment-driven flux and an additional interlayer transfer [the $\hat{F}_i^{(\theta,S)}$], which is a property of the interface. These interlayer transfers prove to be enormously useful in general; for the moment their use as a convection parameterization will be discussed.

In general terms, if buoyancy is withdrawn through the surface, as it will be during convective events, the overall density of the surface layer will increase. This will be reflected in a layer model by a thickness increase of the denser layers relative to the more buoyant layers. Other considerations aside, such a thickness change can be driven by a negative entrainment rate for E_i^l or a positive one for E_{i+1}^u. The former can be objected to for the physical reasons mentioned above. The latter can be realized if the surface buoyancy flux is ''exported'' to the second layer and used to drive E_{i+1}^u. We achieve this by setting $F_o^{(\theta,S)} = \hat{F}_i^{(\theta,S)}$ in the surface layer. Invoking the coordinate definition constraint in (4) for layer $i + 1$ and using the generalized fluxes in (15) yields a contribution to E_{i+1}^u of

$$\delta E_{i+1}^u = -\left[\frac{\alpha F_o^\theta - \beta F_o^S}{\Delta_i[\rho]}\right], \tag{16}$$

which is seen to be positive. The above is added to the background entrainment defined by (9) to yield a net entrainment:

$$E_i^u = E_{io}^u + \delta E_i^u. \tag{17}$$

The entrainment contribution in (16) has the dual effects of adding a thickening trend to the denser layer and driving downgradient entrainment heat and salt transports via (10). Both are as desired.

d. Penetrative solar radiation

We also need a mixing scheme that can accommodate penetrative solar radiation, which acts as in internal heat source in the upper ocean. The behavior of solar radiation in the subsurface ocean is a strong function of wavelength, and is often written

$$I(z) = \int_\omega I_o(\omega) e^{-z/\lambda(\omega)}\, d\omega, \tag{18}$$

where $\lambda(\omega)$ is the attenuation length of the radiation with wavelength ω. The incident radiation amplitude at the surface ($z = \eta$) is I_o, also a function of ω, and the integral is over all radiation wavelengths. For many purposes, it is adequate to approximate (18) using

$$I = I_o(0.6e^{-z/\beta_1} + 0.4e^{-z/\beta_2}), \tag{19}$$

where I_o now represents the total radiative energy flux, β_1 and β_2 the long-wave and short-wave extinction coefficients, and the factors 0.6 and 0.4, the fractions of total radiation in long- and short-wave portions of the spectrum (Kraus 1972). Typical values for β_1 and β_2 are 0.6 and 20 m, respectively (Paulson and Simpson 1977; Price et al. 1986). We will adopt the above formula whenever necessary.

In any case, it is convenient to write the temperature equation in the general form

$$\frac{d}{dt}\theta_i = -F_{iz}^\theta - F_{iz}^R, \tag{20}$$

where the radiative source ($F_i^R = -I_i$) has been written separately from the turbulent fluxes. When (20) is integrated over a layer and the requirement that θ_i be vertically well mixed is enforced, the result is

$$h_i \frac{d}{dt}\theta_i = -F_i^{\theta,u} + F_i^{\theta,l} - \delta F_i^R, \tag{21}$$

where the last term measures the net radiative heating in layer i.

The interlayer transfers as convective parameterizations permit the immediate inclusion of penetrative radiation in a layered model. Radiation represents a positive definite buoyancy input into the subsurface; therefore, it drives a tendency for subsurface fluid to convect upward as a buoyant fluid. Including a contribution to the interlayer transfers of the form

$$\delta\hat{F}_{i-1}^\theta = -\delta F_i^R \tag{22}$$

exports the layer i radiative input to the layer above, which may then thicken proportionally (by means of a positive definite contribution to the entrainment E_{i-1}^l) and reflect the warming. Note that the heat and salinity

budgets each must be balanced separately and that penetrative radiation has no immediate effect on salinity. Thus (22) applies independently of the salinity structure.

e. Restratification

At the transition from late winter to spring, surface mixed layers go from deep, well-mixed convective layers to shallow, entraining and warming layers. Analogous but smaller-amplitude transitions occur during the formation and destruction of the diurnal mixed layer. While the disappearance of interior layers against the boundary, driven by diffusion or convection, is straightforward, the above scenarios imply the need in a layered fluid for a consistent prescription for generating new, more buoyant layers. The dynamic description of the one-dimensional evolution in (1)–(3) demonstrates that a complete specification of an initial layer upon its appearance requires knowledge of the new layer θ_i, S_i, and E_i^l, as well as recognition of the conditions under which a new layer is required. The resolution of these issues is now discussed.

Assuming the latter condition is met, that is, it is recognized at a given time that a new layer is required, the three necessary degrees of freedom can be specified by the appropriate forms of (1)–(3). First, for $h_i = 0$, it is recognized that the integrated forms of (1) and (2) [i.e., (5) and (6)] become

$$0 = -F_o^{(\theta,S)} + F_i^{(\theta,S),l}, \tag{23}$$

where the surface fluxes are assumed known. Multiplying the temperature equation by $-\alpha$, the salinity equation by β and adding yields the result

$$E_i^l = \left[\frac{\alpha(F_o^\theta + \delta F_{i+1}^R) - \beta F_o^S}{\Delta_i[\rho]}\right], \tag{24}$$

where the presence of penetrative solar radiation has been made explicit. Equation (24) specifies one of the needed degrees of freedom and permits the time evolution of the new layer thickness to be calculated via (3). Insertion of (24) into the special forms in (23) yields

$$\theta_i = \theta_{i+1} - \frac{F_o^\theta + \delta F_{i+1}^R}{E_i^l} \quad \text{and} \quad S_i = S_{i+1} - \frac{F_o^S}{E_i^l}, \tag{25}$$

thus completing the specification of layer properties.

All that is left is to construct the physical rule governing the appearance of a new layer. As we are necessarily discussing entraining scenarios here, the ultimate question is whether adequate energy is available to mix the surface buoyancy flux down to the level of the first interface. If so, a new layer cannot develop; otherwise, a new layer is required. In essence, this is a parameterization of restratification.

There are many ways to decide the answer to this question. Indeed, the Kraus–Turner energy closure at the heart of many mixed layer models considers essentially this point. Other approaches are to be found in Pollard et al. (1973) and Price et al. (1986), but again one of the salient issues is the energy available for mixing versus the stabilizing input of buoyancy by surface fluxes. For the proposed structure of our density field, the relevent energy balance involves the Monin–Obhukov length. Specifically, knowing the buoyancy flux, B_f, and the wind stress, $\boldsymbol{\tau}$, Monin–Obukhov scaling predicts wind mixing in an unstratified fluid to a depth of

$$h_{\text{mo}} = \frac{u_*^3}{B_f}, \tag{26}$$

where $u_* = \sqrt{|\boldsymbol{\tau}|/\rho}$ is the friction velocity of the wind stress. Here we have chosen the specific value $\kappa = 1$ for κ in (9). We monitor the quantity h_{mo} and create a new layer in the dual event that the first nonzero thickness interface is at a depth greater than h_{mo} and the associated surface fluxes generate a surface density lighter than the uppermost density. The latter consideration arises due to the discrete density resolution of the model and will be discussed in a later section on sea surface temperature.

f. Details

Last, to produce a stable code, it has been necessary to provide for extreme cases, such as when a newly created layer is extremely thin (e.g., 10^{-5} m). If the standard formulas are used, small errors in the flux differences, when divided by the small thickness, can lead to large errors in the associated tracer time derivatives. Techniques for controlling these instabilities have been proposed by Hallberg (2000). We have taken a simpler route here, and artificially set the time derivatives to zero for very thin layers. Upper-layer entrainments are computed using the net radiative input from layer $i + 1$, but the remaining buoyant fluxes that would otherwise generate nonzero temporal tracer derivatives are exported via the interlayer fluxes to the next layer down. This is done until the upper-layer thickness exceeds a minimum preset thickness (in the runs to be shown, this was 1 m). The overall model behavior seemed to be rather insensitive to the exact choice of this parameter, as long as it was small. It is important to note that the exact conservation of all tracers is still enforced by this procedure, so no spurious contributions to salinity or heat result.

The technique for generating new layers had to be generalized to work on the bottom, for the reason that convection can reach all the way through the fluid column. Under these circumstances, it is necessary to create a new denser water mass. The procedure described above for creating a new, lighter water mass under entraining conditions proved to generalize simply to full-column convective situations.

Finally, when interior layers are lost to the boundaries via diffusion or convection, the model can predict negative thickness. These are removed by adjusting the interface neighboring the boundary such that mass, heat,

and salt are conserved. These three constraints, plus the coordinate constraint, are sufficient to determine the four variables of the problem (i.e., θ_i, S_i, h_i, and h_{i+1}, where i is the index of the new upper layer). The quantities θ_{i+1} and S_{i+1} are not altered during this adjustment. Minor changes to this prescription occur for the special cases in which their are only one or two layers total in the fluid.

3. Numerical examples

The previous section describes the internally consistent development of a surface mixed layer representation in density coordinates. It possesses the properties of exact conservation of heat and salt, physically acceptable downgradient fluxes, can accommodate penetrative solar radiation, and permits arbitrary boundary data. In this section, the model is tested against the well-known Price et al. (1986) mixed layer model (PWP hereafter), with the objectives of addressing model skill and behavior characteristics.

The PWP model is based loosely on Pollard et al. (1973) and computes mixed layer characteristics given surface fluxes of heat, salt, and momentum. Mixing is computed by considering the gravitational and dynamical stability of the layer. For example, buoyancy extraction generates convective mixing down to a depth at which neutral stability is achieved. The momentum input from the wind generates a flow (mainly inertial oscillations) that can develop a shear across the mixed layer base. This flow is gauged for its stability via a bulk Froude number criteria; if unstable, the mixed layer mixes downward until stability is achieved. Finally, the entire profile is readjusted according to a local Richardson number stability criterion. The accuracy of this model has been demonstrated by comparison with observations from the Pacific Ocean (Price et al. 1986) and it has seen broad use as a result.

Here, we compare predictions from the PWP model subject to the standard momentum and buoyancy forcings, and slightly modified versions of those forcings, contained within the freely available source code. These same forcings were also used to drive the present density coordinate mixed layer model. The standard forcing of the PWP model consists of diurnally varying solar radiation divided into short- and long-wave length contributions as in (19). The peak radiation value is 978 W m^{-2} and its amplitude grows from zero to a maximum at noontime and diminishes again during the progression from sunrise to sunset. Nighttime is characterized by a vanishing solar radiation, and throughout the day the ocean surface emits a constant long wave radiative upward heat flux at a rate of 126 W m^{-2}. Salinity forcing is available by specifying the net freshwater flux, but in the standard forcing of the model, this is set to zero. The model can accommodate sub–mixed layer background diffusion, although the default value is zero. In the comparisons to be shown, the diapycnal diffusion coefficient has been set to 2×10^{-5} m^2 s^{-1}, similar to that suggested by the NATRE results reported in Ledwell et al. (1993). A constant zonal wind stress of 0.07 Pa (equivalent to a friction velocity of 0.0085 m s^{-1}) is applied and a vertical resolution of 1 m has been chosen. Conversion from watts per meter squared to a temperature flux employs a heat capacity of 4183 J (kg K)$^{-1}$ and an average density of 1024 kg m^{-3}. The thermal expansion and saline contraction coefficients were set to $\alpha = -2 \times 10^{-4}$ K^{-1} and $\beta = 8 \times 10^{-4}$ PSU^{-1}. The standard initial profiles of the PWP model are uniform salinity at 36 PSU^{-1}, a constant temperature of 20°C to 50 m and linearly decreasing temperature after that to a minimum of 5°C at a depth of 200 m.

The basic parameters of our density coordinate model are that uniform density steps of 4×10^{-1} kg m^{-3} between layers are used, the average density was 1000 kg m^{-3} and the interior layers are subject to an effective diffusivity of (2–4) $\times$ 10^{-5} m^2 s^{-1}. The background diffusivity coefficient employed in the lower of the two surface layers was effectively (0.5–1.0) $\times$ 10^{-3} m^2 s^{-1}. The initial profiles for the density coordinate model were uniform salinity at 36 PSU and a 50-m upper layer at 20°C. Uniform temperature steps of 2°C were employed after that with layers of uniform 20-m thickness, down to a maximum depth of 190 m and a minimum temperature of 6°C. Also, in several of the upcoming comparisons, we have not monitored any of the sea surface properties, which has the effect that the introduction of a new surface layer under entraining scenarios depends only on the condition that the Monin–Obhukov length scale is less than the depth of the first interface.

The results of typical year-long calculations using time steps of 30 min appear in Fig. 4. The temperature profiles versus depth at 60-day intervals appear in the successive subpanels. The PWP model results appear as the smooth lines and the density coordinate model as the steppy lines. The nature of the forcing in this problem is that over long intervals considerable net buoyancy is added to the system. This is at least partly due to the lack of a seasonal cycle in the solar radiation and appears in the warming trend evident in both models. The net heat added agrees for both models to three digits, at 978 K m.

The persistent warming trend in the PWP model is punctuated by occasional mixing events. These are due to a joint effect of the inertial oscillations in the model and the deepening. Specifically, the momentum in the mixed layer and just under the mixed layer can occasionally become out of phase, thus inducing a large shear. This can, by the Froude number mixing mechanism, initiate a burst of deepening. These are not captured by the density coordinate model whose mixing depth representation is considerably simpler. Nonetheless, the year-long trends are faithfully represented.

Examples of the shorter timescale behavior appear in Fig. 5. This is a close look at the mixed layer behavior

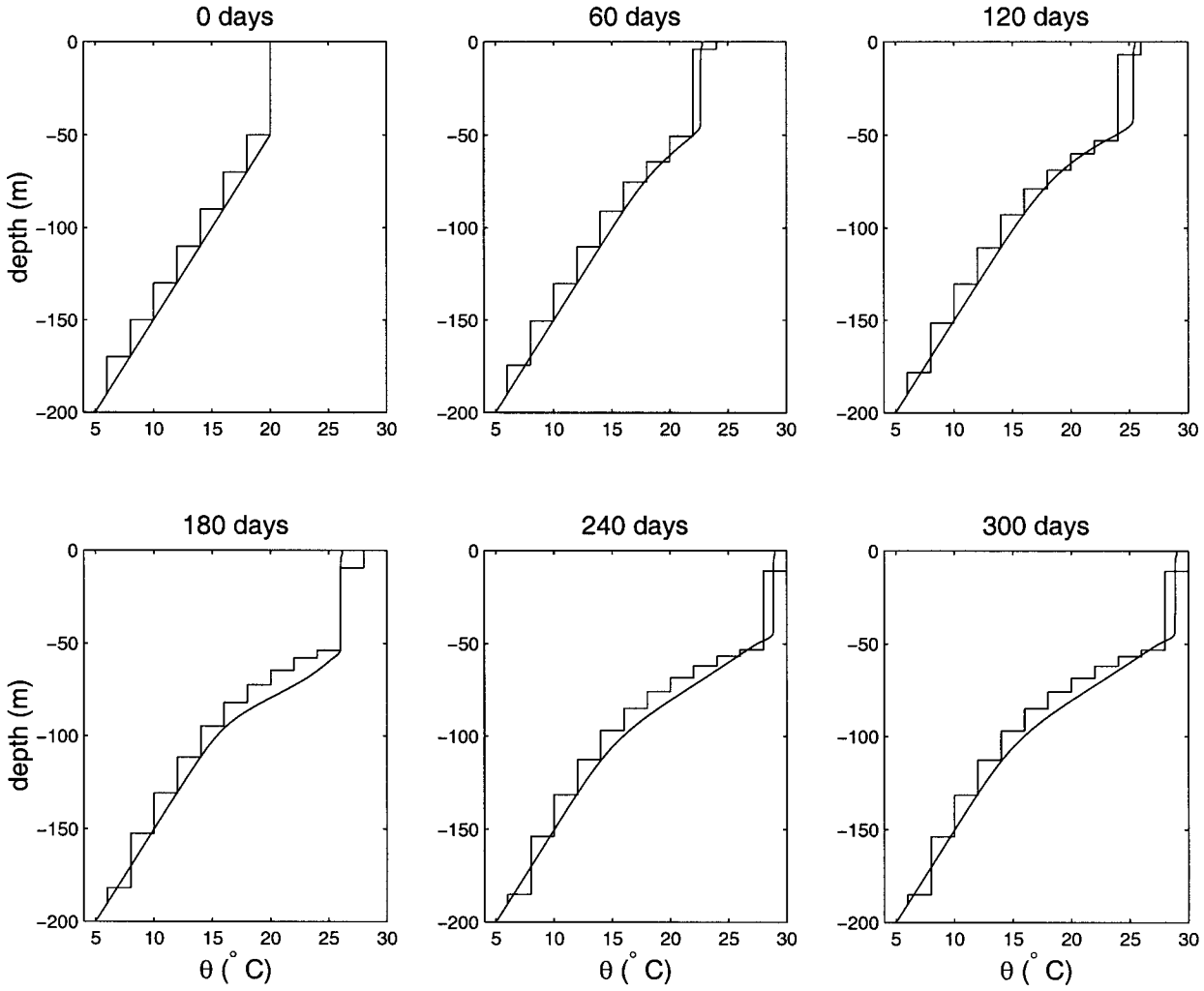

FIG. 4. A comparison of the PWP mixed layer model and the density coordinate model. The temperature–depth plots for a 200-m-deep column are shown at days (a) 0, (b) 60, (c) 120, (d) 180, (e) 240, and 300 (f). Salinity is initially constant at 36 PSU and remains so throughout the run. The smooth curve is from the PWP model and the broken curve from the density coordinate model.

over one day, broken up into roughly 4-h intervals. The density field in this experiment differs from the previous experiment, in that the temperature interval between layers is finer at 0.5°C (in the experiment in Fig. 4, $\Delta\theta = 2$°C). Other parameters are identical to those in the previous run. The sequence begins at midnight and comes from results roughly 6 months into the run. The first panel shows a convectively overturning mixed layer, the convection being driven by the late-night longwave cooling of the surface. The small density step at about 3 m in the midnight PWP results is indicative of an eroding diurnal mixed layer and the convection in the density coordinate model is revealed in the upper three panels by the shallowing of the interface. Convection persists through the next two plots for both models, but by shortly after 0800 local time (LT), incident radiation has begun to inject buoyancy into the mixed layer. A thin surface intensified diurnal thermocline forms in both models over the next two panels. A deepening event associated with the diurnal jet occurs at roughly noontime in the PWP results and this is missed in the density coordinate model. For that reason, the 1100 LT results, rather than the noon results, are shown. The diurnal restratification in the density coordinate model appears in the generation of a new 27°C layer by 1100 LT. By 2000 LT, convection is again eroding the stratification. In all, the qualitative features of the diurnal mixed layer cycle show up in the density coordinate model. There is also skill evident in the quantitative predictions of the density coordinate model.

In general, one expects the buoyant forcing of the mixed layer at a fixed location to input less net buoyancy over a year than characterizes the experiment of Fig. 4. An example of the density model behavior subject to such forcing appears in Fig. 6 where comparisons with the PWP model are again given. The density resolution

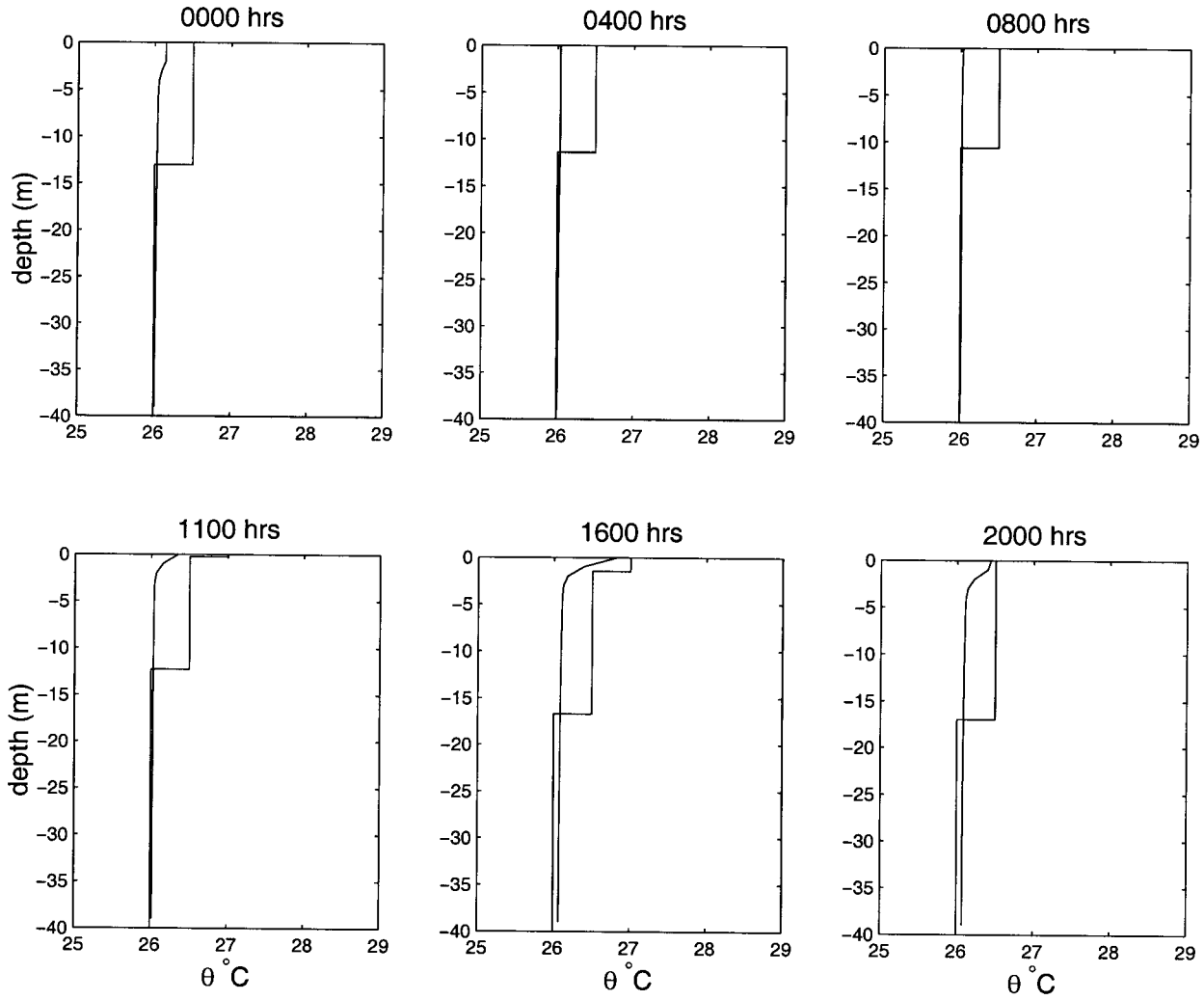

FIG. 5. A comparison of the PWP mixed layer model and the density coordinate model. The temperature–depth plots for a upper 200-m-deep column are shown at 4-h intervals from day 180 of the 1-yr-long run: (a) $t = 0000$, (b) $t = 0400$, (c) $t = 0800$, (d) $t = 1100$, (e) $t = 1600$, and (f) 2000 h. The smooth curve is from the PWP model and the broken curve the density coordinate model. Note the formation of the surface-trapped diurnal thermocline.

of this model has again been set to a constant, equivalent to 2°C temperature steps. Here, incident solar radiation has been turned off and the surface temperature flux in both models is computed according to

$$F_o^\theta = \frac{\mu\{\theta - [20 + 10\cos(2\pi t\ \mathrm{yr}^{-1})]\}}{\rho_w C_{pw}} \qquad (27)$$

where $\mu = 35$ W (m^2 °C)$^{-1}$ is an exchange coefficient like that used in many ocean-only (Haney 1971; Frankignoul 1985) and coupled climate (Saravanan and McWilliams 1998) studies. The quantity $C_{pw} = 4183$ J (kg K)$^{-1}$ is the heat capacity of water and $\rho_w = 1024$ kg m^{-3} an average ocean density. The quantity θ in (27) is the model surface temperature, the calculation of which for the density coordinate model is discussed in section 3a. The setup of the PWP model is standard, aside from the lack of insolation and the use of persistently light winds. The reasons for the latter modification to the PWP forcing are also explained in section 3a on sea surface temperature. The models were run for 20 yr, by which time the response was largely periodic. What is shown is the last year of the run. Each of the panels is labeled with a month representative of the Northern Hemisphere phase of the buoyancy forcing. The overall qualitative behavior is intuitively pleasing, with later winter characterized by deep convectively driven mixed layers, and the summertime by strong thermoclines. The transitional spring and autumn seasons are consistent with thermocline development and erosion, respectively. In addition, the character of the thermocline computed by the density coordinate model agrees relatively well with that predicted by the PWP model.

Last, we compare the results of a run in which the

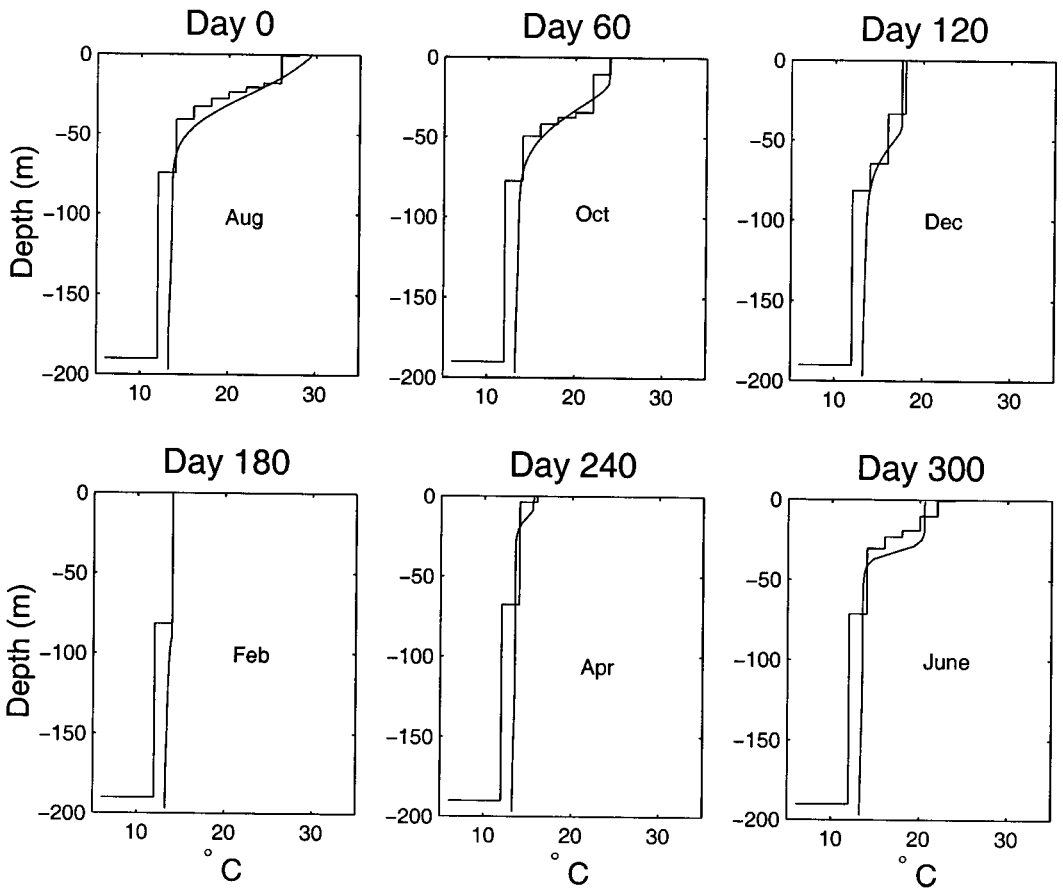

FIG. 6. Mixed layer behavior under seasonal forcing. Here incident radiant solar forcing has been neglected. The surface buoyancy flux is determined by relaxation toward an equilibrium temperature between 10° and 30°C varying sinusoidally with the annual frequency. The relaxation coefficient is 35 W (m^2 °C)$^{-1}$. The present density coordinate model (the stepped line) is compared to the PWP model (the smooth line) forced in the same way. Six different snapshots that span the 20th year of 20-yr runs are shown. Note that the strong late summer stratification is eroded by convection and that the subsequent spring is characterized by restratification in the near surface.

mixed layer receives heat, penetrative solar, and freshwater forcing. In this case, temperature and salinity are both variable but in the density coordinate model must always be related via the equation of state to a prespecified density value. The standard heat flux forcing of the PWP model is employed, but the net freshwater flux is set to

$$e - p = 1 \frac{\text{m}}{\text{yr}} \cos(2\pi t \text{ yr}^{-1}) \tag{28}$$

with a 2-m peak to trough variation and net zero freshwater input. For comparison, the Atlantic Ocean is a net evaporative basin on annual average at about 0.37 m yr^{-1} (Baumgartner and Reichel 1975). The peak to trough range of both the evaporative and precipitation cycles at roughly 20°N are about 1 m, but reasonably in phase, so that the annual ($p - e$) range (sometimes called the runoff rate) is typically less than 1 m. Our test case is then a reasonably strongly forced one from a freshwater anomaly perspective. The model starts from the same initial profile, and uses the same parameters, as the temperature-only run in Fig. 4, and has a uniform salinity set at 36 PSU.

The temperature profiles look similar to those in Fig. 4 and are not repeated here; rather, we show the developing salinity profiles in Fig. 7. The same format is used as for Fig. 4; that is, temporal intervals of roughly 60 days are portrayed and results from both models appear. Note the initial halocline development of the mixed layer in the upper panels of the plot, consistent with the excess of evaporation over precipitation. Subsequent evolution is controlled by the precipitation driven freshening of the surface. It is also interesting to observe the downward penetration of the salinity signal into the interior, driven by the combination of mixed layer deepening and retreat and interior diapycnal diffusion. Note as well that the qualitative and quantitative behavior of the salinity compares well in both models. The total salt has remained constant in the density coordinate model, and changed only very slightly in the PWP model (owing to the lack of a free surface in the PWP model).

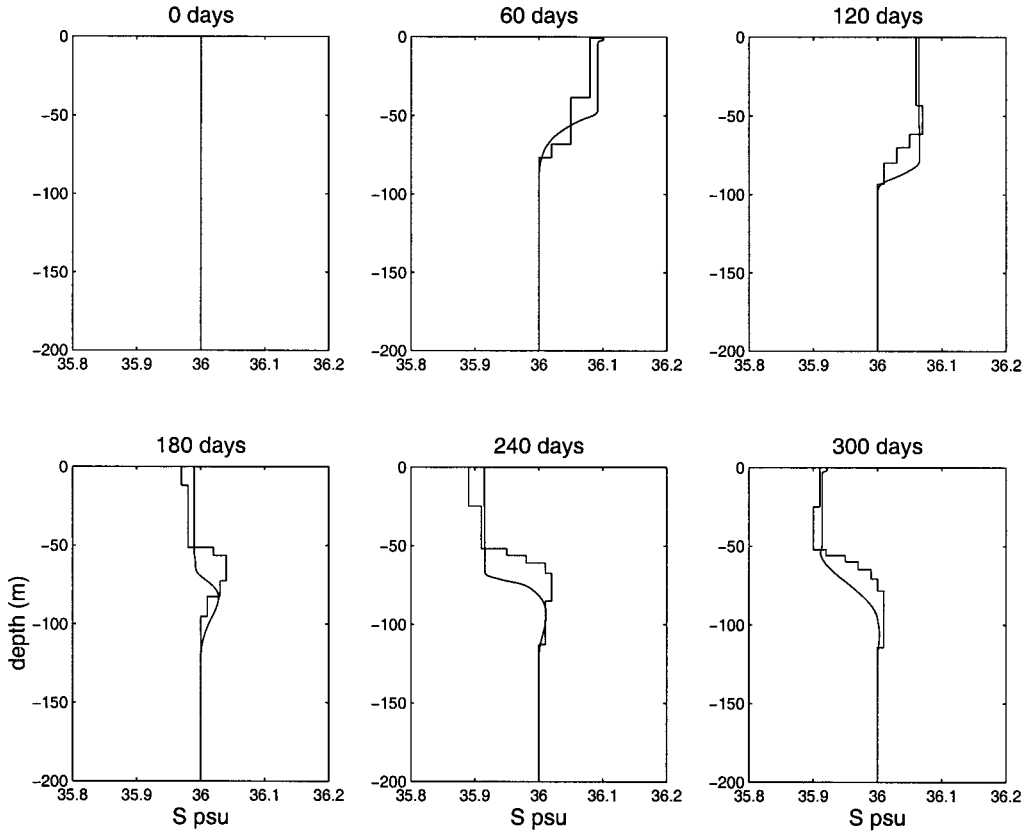

FIG. 7. Salinity profiles from a heat and freshwater forced model run. The plot format is the same as Fig. 4 except salinity is shown.

The density fields of the models are compared in Fig. 8 at the same time intervals. Note that the overall structural comparison is very good here, indicating density coordinate model skill in predicting the mixed layer density structure.

a. Sea surface temperature

An ocean variable of considerable importance, particularly in climate applications, is sea surface temperature (SST), because SST is used to compute ocean–atmosphere exchanges. A major issue for mixed layer models made from discrete densities to address then is the construction of a well-behaved SST. The most obvious SST choice, that is, the temperature of the layer at the surface, can suffer from discontinuity in time. To see this, consider a model stratified in temperature only. Then temperature and density are synonymous, and the surfacing or creation of a layer at the surface would generate a surface temperature different by the model temperature step than that that occurred at the previous step. Equally problematic is the property that SST would remain fixed until the next layer surfacing or creation event took place.

Here we describe the construction of a surface temperature variable from the present density coordinate model that does not suffer from these drawbacks. Rather, the surface temperature is smooth in time and not locked to the predetermined density intervals, even for the extreme case of no salinity stratification. In developing the temperature, care has been taken to base the temperature calculation on density coordinate model variables, as opposed to computing new variables that are outside of the density coordinate construction. Every effort has been made to base the SST estimate on physical considerations, but it should be realized that there is some freedom involved in the procedure discussed here. The technique is likely not to be the optimum procedure, but does serve to demonstrate that a well-behaved ocean surface temperature can be diagnosed from the density coordinate model and that its properties are quite like those computed in models like the PWP model. The philosophy underpinning the procedure is that it is the upper two surface layers that are viewed as modeling the mixed layer. Therefore, the ocean surface temperature is computed from considering the upper two layers.

b. Entrainment scenarios

Consider first the case where buoyancy is being added to the ocean. Wind mixing is then responsible for dis-

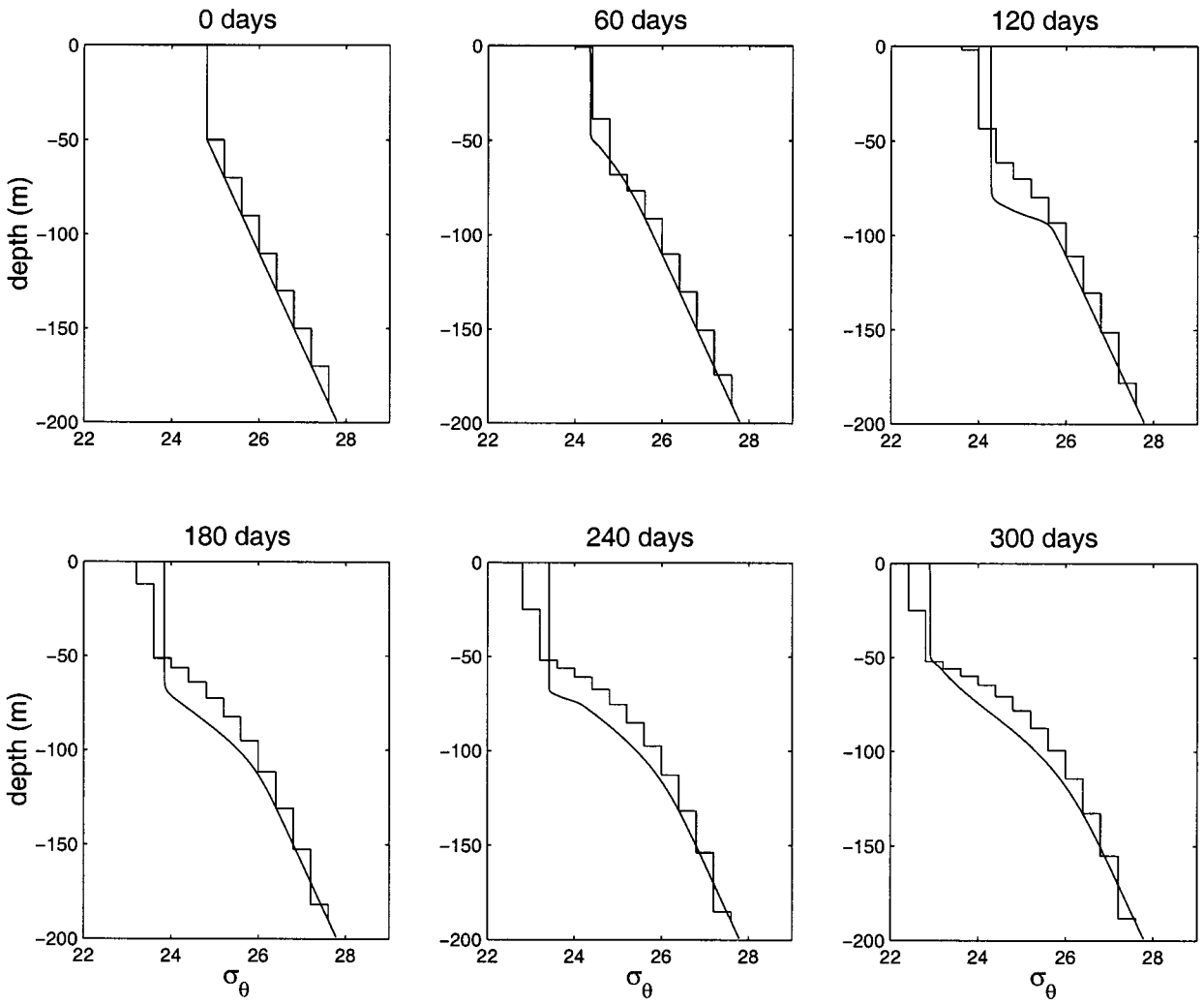

FIG. 8. Mixed layer density from a heat and freshwater forced model. The plot is the same as Fig. 4 except density is shown.

tributing the added buoyancy over the surface. For the surface density structure computed by this model (i.e., two well mixed layers), it is literally the case that the Monin–Obhukov length scale, defined by (26), is pertinent. Two circumstances can arise. First, h_{mo} can be less than the depth of the first interface (see Fig. 9a). The surface fluxes of salinity and heat are then mixed over the depth h_{mo} and used to estimate new surface temperatures and salinities according to the formulas

$$\theta_s = \theta_{\mathrm{old}} - dtF_o^{\theta}/h_{\mathrm{mo}} \quad \text{and} \quad S_s = S_{\mathrm{old}} - dtF_o^{S}/h_{\mathrm{mo}}, \qquad (29)$$

where dt denotes the model time step and θ_{old}, S_{old} the current surface temperature and salinity. In Fig. 9a, salinity is assumed constant and θ_{old} is written as θ_1. The property estimates in (29) are then fed through the equation of state to estimate a new surface density. If the estimated density is lighter than the current surface density (see below), a new layer is created. If not, new layer creation is suppressed, and the first interface is adjusted as if the Monin–Obhukov length scale was greater than the first interface depth. In either case, the new temperature and salinity defined by (29) become the surface layer properties used for computing surface property fluxes.

The reason for this cautious approach is that the density coordinate model uses the two surface layers for the mixed layer, and thus conceptually, the mixed layer density is a weighted average of the upper two layers. Therefore, the ''mixed layer density'' will often be denser than the target density of the topmost layer. The buoyancy due to surface forcing added at any one time may not be sufficient to create water of the next more buoyant layer. The present approach has therefore been designed to constrain the surface properties to belong to the interval of the surface layer.

A second possibility is that h_{mo} is greater than the depth of the first interface (see Fig. 9b). This says that the buoyancy fluxes will be mixed beyond h_1; however, the Monin–Obhukov depth is not in this case the rele-

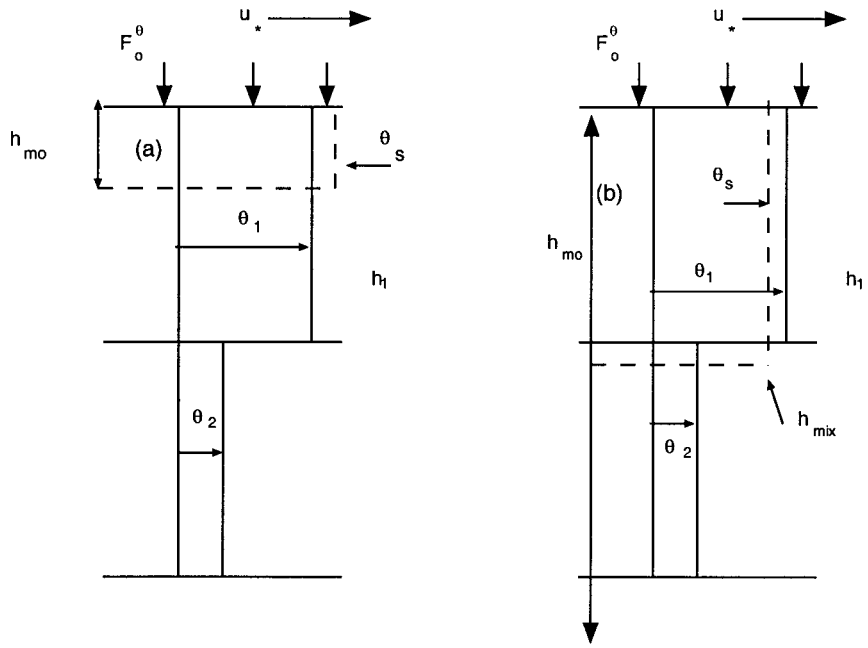

FIG. 9. Mixing schematic. A very shallow Monin–Obhukov length scale appears in (a). New surface properties are computed by adding the surface fluxes mixed over this scale to the old properties. The resulting temperature is shown by the dashed line and is labeled θ_s. A deep Monin–Obhukov scale appears in (b). The depth over which the layer temperatures is averaged is computed from the current interface depth augmented by a turbulent mixing contribution. The result is labeled as h_{mix} (appearing as the horizontal dashed line) and the resultant surface temperature is shown by the vertical dashed line and labeled θ_s.

vant mixing depth because of the presence of the density step associated with the first interface.

To examine how the mixing would proceed, consider the simple case depicted in Fig. 9b of a two-layer fluid stirred by wind-driven turbulence from the top (at a rate of u_*^3) and governed by

$$h\theta_t = -F_o^\theta + e(\theta_2 - \theta),$$

$$h_t = e, \quad \text{and}$$

$$g\alpha(\theta_2 - \theta)h_t = u_*^3 + g\alpha F_o^\theta h. \tag{30}$$

Here it has been assumed the fluid is stratified in θ only, θ_2 is the temperature in layer 2, and all notation is as shown in Fig. 9b. Given initial conditions on h $(=h_1)$ and θ $(=\theta_1)$, the solution for $h_{\text{mix}} = h(t)$ from (30) is

$$h_{\text{mix}} = h_{\text{mo}} + \frac{h_1 - h_{\text{mo}}}{1 - \dfrac{F_o^\theta t}{h_1 \Delta\theta}}, \tag{31}$$

where t is time and $\Delta\theta = \theta_1 - \theta_2$. The quantity h_{mix} is the depth to which the wind stirring will mix the fluid. The formula generalizes to a fluid stratified in temperature and salinity by replacing the temperature flux by the net buoyancy flux and the temperature step by the buoyancy step.

If we identify the initial depth and temperature with those from the upper layer of the model at a given time, and the total time t with the time step of the model, (31) provides an estimate of the depth over which the surface fluxes will be mixed over a model time step. Thus, we diagnose surface properties by averaging the model properties over the depth h_{mix} from (31).

c. Convecting scenarios

The only remaining possibility is that the fluid is convecting. For convection, we average the mixed layer properties over the depth used in the previous time interval. This depth remains fixed unless the convection completely removes a given interface from the fluid. In this case, the averaging depth is set to the depth of the next interface.

These rules are sufficient to define surface ocean properties under all conditions, and have the advantage that they are based in simple models of mixing. They also appeal to the density coordinate mixed layer model variables and thus fit simply within the framework discussed here.

We show in Fig. 10 comparisons of the SST computed by our density coordinate mixed layer model and that computed using the PWP model. This experiment was initialized in the same way as that shown in Fig. 4 for both the PWP and the density coordinate models. Note, this is a fluid stratified in temperature only, a test purposely conducted because the temperature structure of

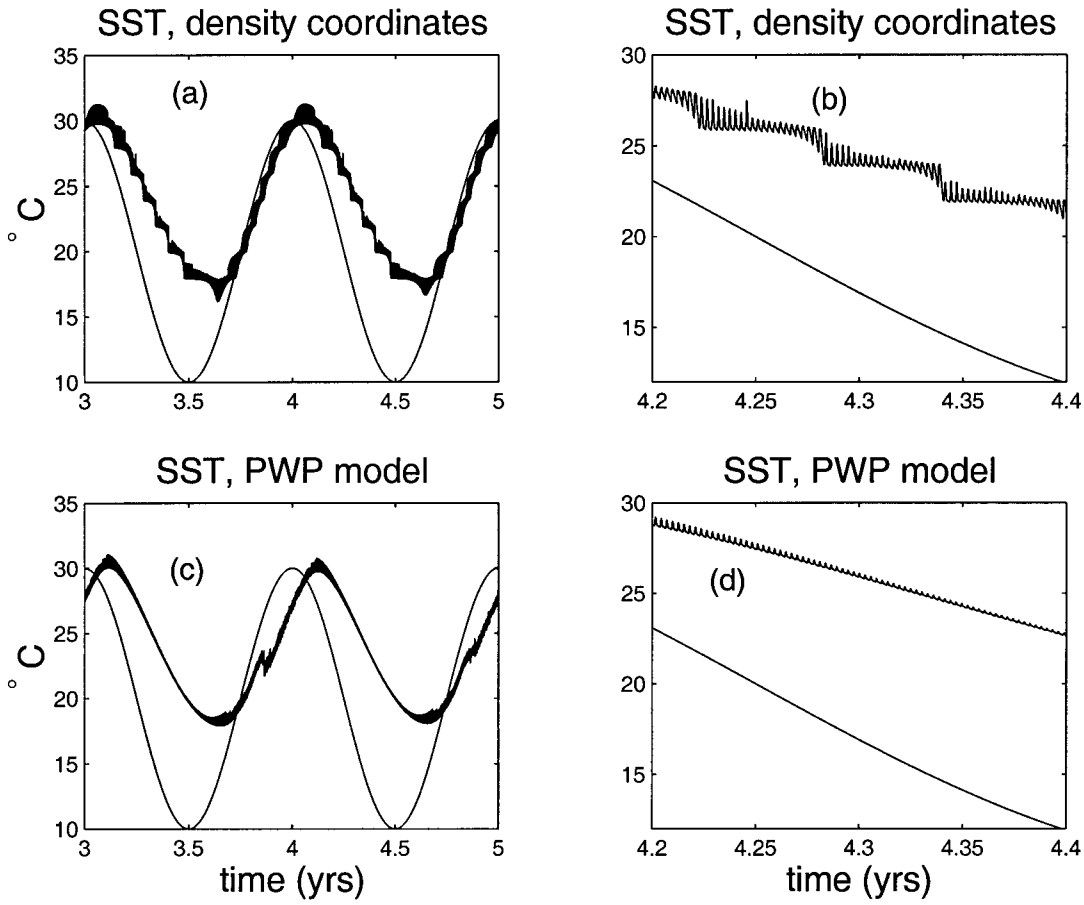

FIG. 10. A comparison of SST computed from the density coordinate model and from the PWP model. The last 2 yr of a 5-yr run are shown in (a) and (c). The smooth line common to both plots is the background temperature to which the ocean is relaxed. Magnified views of the convecting phase in year 4 appear in (c) and (d). The comparison is quite good between the amplitude and phase of the SSTs from both models.

the density coordinate model is guaranteed to be discontinuous. If salinity were active, the temperatures in each layer would vary in time, and the smoothness of the SST could be enhanced. The forcing in this set of experiments is the same as that used for the results in Fig. 6, in that the surface temperatures from the models were fed back into the temperature flux calculations. (Recall that, in the other experiments shown here, fluxes were assumed to be known and imposed as the forcing.) In particular, the temperature fluxes were governed by (27). Both models were then run for a period of 5 yr.

The SSTs from our initial comparison, while qualitatively similar, showed that the PWP model had a smaller range in temperatures and was somewhat slower to respond to the annual cycle than the density coordinate model. This is due to the fact that the PWP uses three mechanisms for deepening the mixed layer: wind-driven stirring, convection, and shear-driven mixing. Only the first two are currently included in the density coordinate model; thus the PWP model mixed layers were deeper in the standard configuration and exhibited greater thermal inertia. As a remedy, to permit a more careful comparison, the wind stresses in the PWP model were reduced from 0.07 to 0.02 Pa. Under these permanent light wind conditions, the mixed layer depth differential between the two models was reduced, and the behavior of the density coordinate mixed layer model could be more critically examined.

The comparisons for years 4 and 5 appear in Figs. 10a,c and closeups of the convective period from year 4.2 to 4.4 appear in Figs. 10b,d. The smooth line in all panels is the background target temperature to which the surface temperature is relaxed. The overall comparison in the left-hand panels is quite favorable. Note that the range of both models (roughly 20°–30°C) is about the same and that the phasing relative to the background cycle compares well. The finescale ''hash'' on all these plots is from the daily cycle, and it is seen that the daily temperature range from the models is comparable, especially during warming entraining phases. Convecting (cooling) scenarios have larger daily SST ranges in the density coordinate model. To be sure, the model SST is ''aware'' of the discrete temperature intervals associated with the initial model configuration.

This appears in the tendencies for the SSTs to clump around given temperatures. This is an error associated with the discretization of the model (here $\Delta\theta = 2°C$) and will become smaller with higher resolution (i.e., smaller temperature jumps). The finescale view in the right-hand panels clarifies that the temperature changes during convection are smooth. This plot supports the point that the construction of a smoothly varying SST from a density coordinate mixed layer model is possible. Further, while it is necessary to carry two extra variables (i.e., SST and a sea surface salinity) to store sea surface properties, their calculation appeals only to density coordinate model variables.

4. Discussion

A mixed layer model developed in density coordinates is discussed. The motivation for constructing such a model comes from a desire to eliminate certain physical problems associated with existing attempts to couple classical mixed layer models, which resolve density continuously, to layered interiors, which resolve density discretely. Particularly during the detrainment phases of mixed layers, buoyant anomalies exist relative to the prespecified density classes the interior can accept. This excess buoyancy is moved artificially within the models in order that net heat and salt be conserved. The results of this process can be problematic in important water mass formation zones. Such problems are eliminated if mixed layer models operating only in the predefined density classes of the model are used. The objective of this paper is to develop such a model from first principles and to demonstrate its behaviors.

The basic building blocks of the present model are found in the mixing scheme of MD98, where dual-sided entrainment was suggested as the mixing model. It has been useful, and indeed necessary, to generalize the associated tracer fluxes proposed by MD98 to include an interlayer exchange process. These additional fluxes are properties of the interface and are meant as parameterizations of buoyant convective processes. Their inclusion permits convection to proceed in a density coordinate model via positive definite entrainment rates and, therefore, with physically acceptable downgradient entrainment fluxes. Their use extends beyond that of simple convection to the inclusion of penetrative solar radiation. We have also discussed how restratification processes can be represented within the model and a simple model for calculating mixed layer depths. We suggest that the behavior of this model is qualitatively and quantitatively encouraging. When compared to a well-known and widely accepted classical mixed layer model, the PWP model, the surface behavior in both tracers and density is similar.

Extension of the present ideas from one to three spatial dimension in principle presents no problem. The focus of this paper has been the tracer and continuity equations, and we argue that inserting the above formalism into a full GCM simply increases the inputs to the tracer time derivatives by one. The constraint in (4), necessary to ensure coordinate conservation, is unaffected by advection.

There is also at least one advantage of the density coordinate approach that bears explicit mention. The seasonal, summertime thermocline can be quite sharp. This appears in Figs. 7 and 8 in the model results as the strong S and ρ gradients between 50 and 100 m and in Fig. 6 in the sharp θ gradient between the surface and 50 m. Recall however that the PWP model used here is resolved at 1 m everywhere; it is clear in general that fine resolutions are necessary to accurately capture the summer thermocline. However, the location of the thermocline cannot be predicted in advance, so to ensure that it is well modeled requires fine resolution throughout the upper reaches of the model. The current density coordinate model, however, automatically captures this region of rapid transition due to the quasi-Lagrangian nature of the vertical coordinate. Equivalently, model degrees of freedom are naturally migrated to the thermocline so that it is resolved even with the relatively coarse density spacing of the present model.

There are issues still to be addressed in the full development of a density coordinate mixed layer model. One mentioned above involves the optimal methods for computing when new layers are required to emerge from the surface and the way in which the surface fluxes are distributed over the surface layer. In addition, the model presented here assumes a linear equation of state and subtleties could exist in migrating this procedure to a realistic and fully nonlinear equation of state.

Finally, the focus of this paper has been the tracer equations, and aside from modeling stress driven mixing by means of u_*, momentum has been neglected. One associated drawback has been pointed out; namely, the wind-driven mixing distributing the incoming buoyancy flux across the mixed layer is missing the important element of shear-driven entrainment. An essential extension of these ideas then is to include momentum in the mixed layer equations. While this remains an area of research, the procedure currently being pursued follows similar lines to that discussed here. For example, the vertically integrated zonal momentum equation appropriate to the surface layer of the one-dimensional problem is

$$h_i(u_{it} - f_o v_i) = -\left[\frac{\tau^x}{\rho} + e_i(u_{i+1} - u_i)\right], \qquad (32)$$

where notation is standard and τ^x is the known input of zonal momentum. Mixed layers including the three deepening processes of turbulent mixing, convection, and shear entrainment compute a mixed layer depth evolution during entrainment according to an equation like

$$(|\Delta \mathbf{v}|^2 - g'h)h_t = \lambda(u_*^3 - B_f h) \qquad (33)$$

(Price et al. 1978), where λ is an efficiency parameter

and shear mixing (proportional to the velocity step $\Delta \mathbf{v}$ across the mixed layer base) contributes through the first term on the left-hand side. A key to including this effect in the surface is to compute whether it would drive the mixing deeper than the second interface. If so, the new density coordinate mixed layer properties should be recomputed using the deeper layers with the two target densities bracketing the new mixed layer density. In the process, interior layers may vanish at the mixed layer bottom interface, but this is to be expected as a model of shear-driven entrainment. Entrainment generalizations for vanishing layer inflation due to diffusive processes then govern the recovery of these layers. In all, the procedure is reasonably clear, although many details remain to be addressed.

All of the above issues will be important for the production of a density coordinate model accurate enough to be used for simulation by an ocean-only or coupled climate model system. Nonetheless, the potential isopycnal models hold for global ocean simulation coupled with the possible advantages of a mixed layer construct consistent with an isopycnal interior recommend further study.

Acknowledgments. WKD is supported through NSF Grant OCE-9617728 and NASA Grant NAG5-8291, the latter awarded in support of the NASA Seasonal to Interannual Prediction Project. The author gratefully acknowledges many interesting conversations on this subject with Dr. T. McDougall of CSIRO and Prof. J. Willebrand of the Institüt für Meereskunde, Kiel, Germany. Part of this work was conducted while the author was a visitor to Kiel, and the hospitality of that institution is gratefully acknowledged. The PWP mixed layer source code was kindly provided by Dr. J. Price of the Woods Hole Oceanographic Institution. Sheila Derby assisted in manuscript and figure preparation and Jane Jimeian assisted with computational issues. An anonymous reviewer is thanked for many valuable comments and for requesting the section on sea surface temperature.

REFERENCES

Baumgartner, A., and E. Reichel, 1975: *The World Water Balance.* Elsevier, 179 pp.

Bleck, R., and E. Chassignet, 1994: Simulating the oceanic circulation with isopycnic-coordinate models. *The Oceans: Physical–Chemical Dynamics and Human Impact,* S. K. Majumdar et al., Eds., Pennsylvania Academy of Science, 17–39.

Frankignoul, C., 1985: Sea surface temperature anomalies, planetary waves, and air-sea feedback in the middle latitudes. *Rev. Geophys.,* **23,** 357–390.

Gaspar, P., 1988: Modeling the seasonal cycle of the upper ocean. *J. Phys. Oceanogr.,* **18,** 161–180.

Gent, P., and J. McWilliams, 1990: Isopycnal mixing in ocean circulation models. *J. Phys. Oceanogr.,* **20,** 150–155.

Griffies, S., A. Gnanadesikan, R. Pacanowski, V. Larichev, J. Dukowicz, and R. Smith, 1998: Isoneutral diffusion in a *z*-coordinate ocean model. *J. Phys. Oceanogr.,* **28,** 805–830.

——, R. Pacanowski, and R. Hallberg, 2000: Spurious diapycnal mixing associated with advection in a *z*-coordinate ocean model. *Mon. Wea. Rev.,* **128,** 538–564.

Hallberg, R., 2000: Time integration of diapycnal diffusion and Richardson number–dependent mixing in isopycnal coordinate ocean models. *Mon. Wea. Rev.,* **128,** 1402–1419.

Haney, R., 1971: Surface thermal boundary conditions for ocean circulation models. *J. Phys. Oceanogr.,* **1,** 241–248.

Hu, D., 1996: The computation of diapycnal diffusive and advective scalar fluxes in multilayer isopycnic-coordinate ocean models. *Mon. Wea. Rev.,* **124,** 1834–1851.

Huang, R., 1993: Real freshwater flux as a natural boundary condition for the salinity balance and thermohaline circulation forced by evaporation and precipitation. *J. Phys. Oceanogr.,* **23,** 2428–2446.

Kraus, E., 1972: *Atmosphere–Ocean Interaction.* Clarendon Press, 275 pp.

——, and S. Turner, 1967: A one-dimensional model of the seasonal thermocline: II. The general theory and its consequences. *Tellus,* **19,** 98–106.

Large, W., J. McWilliams, and S. Doney, 1994: Oceanic vertical mixing: A review and a model with a nonlocal boundary layer parameterization. *Rev. Geophys.,* **32,** 363–403.

Ledwell, J., A. Watson, and C. Law, 1993: Evidence for slow mixing across the pycnocline from an open-ocean tracer-release experiment. *Nature,* **364,** 701–703.

McDougall, T., and W. Dewar, 1998: Vertical mixing and cabbeling in layered models. *J. Phys. Oceanogr.,* **28,** 1458–1480.

Murtugudde, R., M. Cane, and V. Prasad, 1995: A reduced-gravity, primitive equation, isopycnic ocean GCM—Formulation and simulations. *Mon. Wea. Rev.,* **123,** 2864–2887.

Niiler, P., and E. Kraus, 1977: One-dimensional models of the upper ocean. *Modelling and Prediction of the Upper Layers of the Ocean,* E. Kraus, Ed., Pergamon, 143–172.

Oberhuber, J., 1993: Simulation of the Atlantic circulation with a coupled sea ice mixed layer isopycnal general circulation model. Part I: Model description. *J. Phys. Oceanogr.,* **23,** 808–829.

Paulson, C., and J. Simpson, 1977: Irradiance measurements in the upper ocean. *J. Phys. Oceanogr.,* **7,** 952–956.

Phillips, N., 1951: A simple three-dimensional model for the study of large-scale extratropical flow patterns. *J. Meteor.,* **8,** 381–394.

Pollard, R., P. Rhines, and R. Thompson, 1973: The deepening of the wind mixed layer. *Geophys. Fluid Dyn.,* **3,** 381–404.

Price, J., C. Mooers, and J. van Leer, 1978: Observation and simulation of storm-induced mixed-layer deepening. *J. Phys. Oceanogr.,* **8,** 582–599.

——, R. Weller, and R. Pinkel, 1986: Diurnal cycling: Observations and models of the upper ocean response to diurnal heating, cooling, and wind mixing. *J. Geophys. Res.,* **91,** 8411–8427.

Saravanan, R., and J. McWilliams, 1998: Advective ocean–atmosphere interaction: An analytical stochastic model with implications for decadal variability. *J. Climate,* **11,** 165–188.

Schopf, P., and A. Loughe, 1995: A reduced-gravity isopycnal ocean model: Hindcasts of El Niño. *Mon. Wea. Rev.,* **123,** 2839–2863.

Veronis, G., 1975: The role of models in tracer studies. *Numerical Models of the Ocean Circulation,* R. Reid, A. Robinson, and K. Bryan, Eds., National Academy of Sciences, 133–146.